Soil Dynamics and Earthquake Engineering 30 (2010) 1–7

Contents lists available at ScienceDirect

Soil Dynamics and Earthquake Engineering

journal homepage: www.elsevier.com/locate/soildyn

Analytical and numerical study of P-wave attenuation in rock shelter layer

Z.L. Wang [a,b,c,*], H. Konietzky [c], R.F. Shen [d]

[a] Department of Geotechnical Engineering, Tongji University, Shanghai 200092, China
[b] Department of Modern Mechanics, University of Science and Technology of China, Hefei 230027, China
[c] Institut für Geotechnik, Technische Universität Bergakademie Freiberg, Freiberg 09596, Germany
[d] Centre for Soft Ground Engineering, National University of Singapore, Singapore 119260, Singapore

ARTICLE INFO

Article history:
Received 6 December 2008
Received in revised form
4 May 2009
Accepted 5 May 2009

Keywords:
Rock shelter layer
Inclusion
Wave attenuation
Analytical solution
Numerical analysis

ABSTRACT

The protection of underground structures against dynamic loadings has long been a topic of great interest in defense engineering. This paper focuses on the far-field blast-wave propagation and attenuation in rock shelter layer with an inclusion or filled medium. First, the effect of single inclusion on wave attenuation is explored analytically assuming that the interfaces between rock and the inclusion are completely consolidated. The formulae for the strength of total transmitted stress- and velocity-wave after the inclusion are subsequently presented. At last, numerical studies on the attenuation of one-dimensional P-wave in rock embedded with artificial cavity, steel plate and natural joint are carried out. The attenuation rules for various scenarios are discussed in detail in this paper which can provide useful guidelines to the design of intelligent defense structures.

1. Introduction

Civil defense structures are usually constructed beneath the ground to provide protection against the destructive effects of blasts. Apart from the basic objective of preventing failure of the structure itself, a major concern is the dynamic response of the structure, which can have detrimental influences on its occupants and other contents [1–4].

Blast-induced waves due to far-field detonation would evolve into propagation of stress wave in underground media. Such waves dissipate and diffract when hitting obstacles-like artificial inclusions (cavities, steel plates) and natural discontinuities (joints, faults). The wave stress intensity may be greatly reduced after passing these obstacles. This reduction of stress from the peak value is often termed as attenuation [5,6]. In the last few decades, the study of wave attenuation through the defense shelter has been a major subject in connection with the assessment of the safety of underground defense structures subjected to blast loadings [7–13].

Military war really boils down to the contest of 'spear' and 'shield' with civil defense structures falling into the latter category. The development of modern military technology greatly enhances the destructive power and hit rate of new weapons, thus posing great challenges to defense engineering nowadays. The conventional solution is to increase the thickness of the protective layer, but there is a limitation to such thickness increase in practice. Hence, pursuing studies on the efficacy of novel intelligent defense structures on damping, dissipating and decaying blast waves so as to improve their capacity to various kinds of shells, bombs and missiles has been a core subject in the defense engineering in recent years [4,14–16].

One such novel intelligent scheme to achieve high damping and screening functions on stress waves using layered model as proposed by Li et al. [15] is illustrated in Fig. 1. Because the dimension of a defense structure is normally much smaller compared to the distance of far-field blast, the blast waves can be regarded as a uniformly varying load applied to the upper boundary. This layered model essentially consists of three components from top to bottom: a soil cover layer, a protective layer and a supporting layer. The protective layer has two substructures: a shelter layer and a stress distribution layer. The stress distribution layer is adopted to redistribute the stress over a larger region, while the shelter layer, usually making up of rock or concrete block with inclusion, is used for dissipating wave energy or resisting projectile penetration [4,14,15].

The present study explores some critical aspects of the design of intelligent defense structure in blast-resistance field with the aim to provide an in-depth understanding of vibration isolation and shock absorption of rock shelter with filled medium. The effect of single inclusion in rock shelter on wave attenuation is explored analytically assuming that the inclusion and the neighboring rock are fully consolidated. The associated formulae of resultant stress and velocity for transmitted waves are

* Corresponding author at: Department of Geotechnical Engineering, Tongji University, Shanghai 200092, China. Fax: +86 216 5985210.
E-mail address: GeowzL@yahoo.com.cn (Z.L. Wang).

0267-7261/$ - see front matter © 2009 Elsevier Ltd. All rights reserved.
doi:10.1016/j.soildyn.2009.05.004

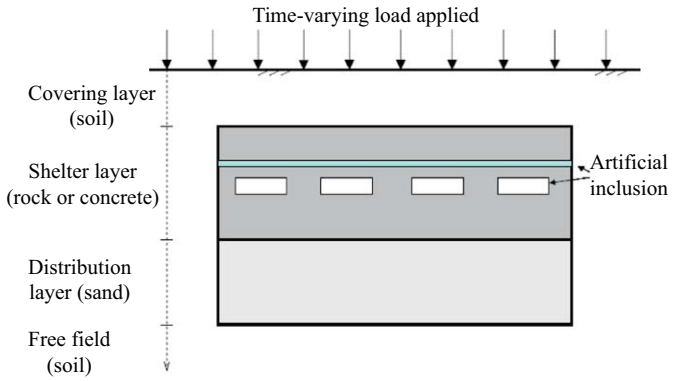

Fig. 1. Schematic of layered defense structure.

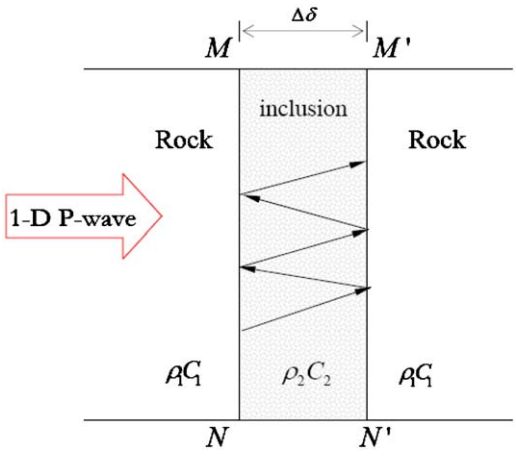

Fig. 2. Wave propagation in rock with inclusion.

subsequently derived. At last, the effects of three kinds of inclusions (cavity, rigid body and joint) on wave transmission and attenuation are numerically investigated in detail and presented in this paper.

2. Numerical tools for simulations

In the present study, the numerical analyses are carried out using LS-DYNA [17] and Universal Distinct Element Code (UDEC) [18]. The latter is instrumental in the simulation of blast-wave propagation in rock with joint inclusion.

LS-DYNA is a general finite element code designed for transient dynamic analysis of highly nonlinear problems. It has a wide variety of analysis capabilities including a large number of material models, a variety of contact options, a large library elements and robust algorithms for adaptively controlling the solution process. The transient analysis is performed using an explicit integration procedure obviating the need for matrix evaluation, assembly and decomposition at each time step as required by many implicit integration algorithms. It automatically examines the finite element mesh and material properties in order to determine an appropriate time step size for numerical stability [17,19].

UDEC is a two-dimensional numerical program for discontinuous system. It is specially developed to model discontinuum subjected to either static or dynamic loading. The discontinuous medium is represented as an assemblage of discrete blocks. The discontinuities are treated as boundary conditions between blocks; large displacements along discontinuities and rotations of blocks are allowed. In other words, the joints are viewed as interfaces between distinct bodies. Individual blocks behave as either rigid or deformable material. Deformable blocks are subdivided into a mesh of finite-difference triangular elements, and each element responds according to a prescribed linear or nonlinear stress–strain law. To model the mechanical interaction between blocks, it is assumed that the blocks are connected by normal and shear elastic springs. The relative motion of the discontinuities is also governed by linear or nonlinear force–displacement relations for movement in both the normal and tangential directions [18].

3. Analytical work of wave attenuation

As shown in Fig. 2, it is assumed that the inclusion is a continuous and homogeneous material with thickness of $\Delta\delta$, and that it is completely consolidated with the surrounding rock at the two-sided interfaces (no separation under tension or compression). When an incident wave (one-dimensional P-wave) is applied normally at the left surface *MN*, disturbances (i.e., the reflected and transmitted waves) will be evoked and subsequently propagate in the rock and inclusion. Based on the theory of stress wave and the Newton's third law, the particle's velocity v and wave stress σ should be equal at both sides of the interface *MN*

$$v_I + v_R = v_T \tag{1}$$

$$\sigma_I + \sigma_R = \sigma_T \tag{2}$$

where the subscripts *I*, *R* and *T* represent the variables associated to incident, reflected and transmitted waves, respectively.

The jump condition of shock waves is given as [5,20]

$$[\sigma] = -\rho C[v] \tag{3}$$

where ρC is wave impedance.

Thus, Eq. (1) can be written by

$$\sigma_I \rho_1 C_1 - \frac{\sigma_R}{\rho_1 C_1} = \frac{\sigma_T}{\rho_2 C_2} \tag{4}$$

Combining Eqs. (2) and (4) yields

$$\sigma_T = \frac{2k}{1+k}\sigma_I = T_\sigma \sigma_I \tag{5}$$

$$\sigma_R = \frac{k-1}{k+1}\sigma_I = F_\sigma \sigma_I \tag{6}$$

where $T_\sigma = 2k/(1+k)$ and $F_\sigma = (k-1)/(k+1)$ are the stress transmission and reflection coefficients, respectively, while $k = \rho_2 C_2/\rho_1 C_1$ denotes the ratio of wave impedances of two materials.

Likewise, when the wave propagates from the inclusion to rock, the following relations hold:

$$\sigma_T = \frac{2}{1+k}\sigma_I = T'_\sigma \sigma_I \tag{7}$$

$$\sigma_R = \frac{1-k}{1+k}\sigma_I = F'_\sigma \sigma_I \tag{8}$$

where T'_σ and F'_σ are the corresponding transmitted and reflected coefficients, respectively.

When the transmitted wave σ_T goes through the inclusion layer, it will be reflected and transmitted at the surface $M'N'$. This will again produces a new return wave, and it will be further reflected when hitting the left interface *MN*. Such reciprocal process goes on until the wave energy is exhausted. By assuming the total number of wave reflections in the inclusion layer is *n*,

thus there are n+1 interaction waves inside [14,21]. It is obvious that the strength of the jth wave can be expressed as

$$\sigma_j = \sigma_T (F'_\sigma)^{j-1} \tag{9}$$

After the interaction of n+1waves in the inclusion, the resultant stress σ within the elastic range can be expressed as [14]

$$\sigma = \sigma_T (1 + a + a^2 + a^3 + \cdots + a^n) = \frac{1 - a^{n+1}}{1 - a} \sigma_T \tag{10}$$

in which $a = F'_\sigma = (1-k)/(1+k)$.

Generally, the total reflected number n depends on the geometry of inclusion layer, the conditions of explosive source, the mechanical properties of rock and the filled material type, etc. The larger the reflection number n, the less the influence of inclusion material on wave propagation is.

If n is an even number, it would have $n/2$ waves transmitted at the surface $M'N'$, whereas there exist $(n+1)/2$ transmitted waves if n is an odd number. The resultant stress of the transmitted waves after the surface $M'N'$ can be expressed as

$$\hat{\sigma} = \begin{cases} \dfrac{1 - a^n}{1 - a^2} b\sigma_I & n \text{ is even} \\ \dfrac{1 - a^{n+1}}{1 - a^2} b\sigma_I & n \text{ is odd} \end{cases} \tag{11}$$

where $b = T'_\sigma T_\sigma$, i.e.,

$$b = \frac{4k}{(1 + k)^2} \tag{12}$$

If the boundary condition is velocity wave, the similar discussions can be made. Under this circumstance, Eqs. (9)–(11) are changed into

$$v_j = v_T (F'_v)^{j-1} \tag{13}$$

$$v = \frac{1 - c^{n+1}}{1 - c} v_T \tag{14}$$

$$\hat{v} = \begin{cases} \dfrac{1 - c^n}{1 - c^2} dv_I & n \text{ is even} \\ \dfrac{1 - c^{n+1}}{1 - c^2} dv_I & n \text{ is odd} \end{cases} \tag{15}$$

where v and v_j are the resultant velocity and the strength of jth reflection in the inclusion layer, respectively; $\hat{v}$ is the total strength of transmitted waves after the surface $M'N'$; $F_v = (T_v - 1)$ and $T_v = T_\sigma/k$ are the velocity-wave reflection and transmission coefficients from rock to filled layer; F'_v and T'_v are the corresponding coefficients in the opposite direction; parameters $c = F'_v = (k-1)/(k+1)$ and $d = b = T_v T'_v = 4k/(1+k)^2$.

The change rules of parameters a, b (or d) and c are graphically illustrated in Fig. 3. It has been found that parameters a and c have the contrary changing trend, while for b and d, the trend is alike. From the above analyses, it can be summarized as:

(i) When $k = 0$, there are $\hat{\sigma} = 0$ and $\hat{v} = 0$. This is the case of complete absorption (without transmission) of waves. If this happens then the effect of inclusion on shock wave attenuation is the most effective.
(ii) When $k = 1$, there exist $\hat{\sigma} = \sigma_I$ and $\hat{v} = v_I$, which corresponds to the complete transmission of waves (without absorption). This is the so-called impedance matching.
(iii) When $k \to \infty$, it would have $\hat{\sigma} = 0$ and $\hat{v} = 0$. This case implies that the inclusion layer is a non-removable rigid body.

It is noteworthy that, in the above discussion, a complete consolidation was assumed between the rock and inclusion. If it is not so, the interfaces MN and $M'N'$ may partially or completely open. For the latter scenario, there will be no waves in the filled layer due to the shock isolation of air in the opening, which may be reduced to the case (i). If the interfaces are partially open, there would exist waves in the inclusion layer. Thus, the effect of interface may be roughly equivalent to the geological discontinuities.

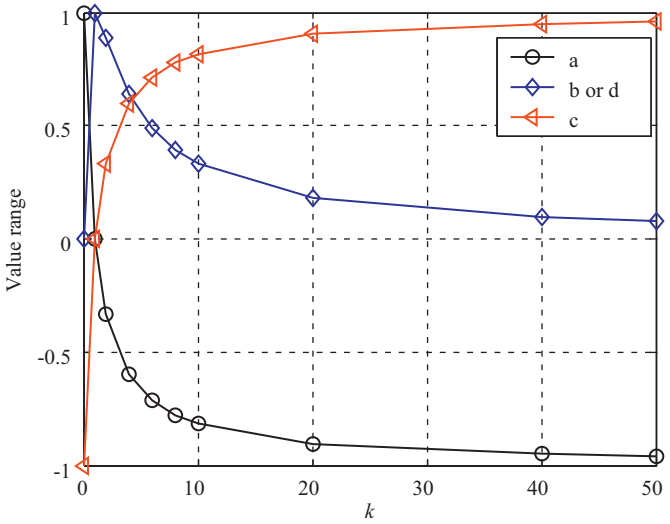

Fig. 3. Change rules of four parameters.

4. Numerical analysis of wave attenuation

As mentioned above, the propagation and attenuation of air-blast induced waves are important considerations in anti-explosion design. In this section, the effects of inclusion material properties on wave attenuation are explored numerically.

For the three scenarios (cavity, rigid body and joint inclusion) to be explored, the specifications of the computational models are similar to each other. In each case, the incident wave is applied normally at the left boundary, and propagates across inclusion layer along the x-direction, as illustrated in Fig. 4. The inclusion is assumed to be located at $x = 50$ cm from the left boundary and is parallel to the both sides of the rock. Non-reflection boundaries are placed at the upper, lower and right boundaries to avoid wave reflections from the artificial boundaries. Blast loading is approximated by the positive part of a complete sinusoidal wave shown in Fig. 5. The wave amplitude and frequency are 100.0 MPa and 5000.0 Hz, respectively.

The rock material is assumed to be linear elastic with the following properties: density $\rho = 2650.0\,\text{kg/m}^3$, elastic modulus $E = 90.0$ GPa and Poisson's ratio $\mu = 0.16$. The properties of three different inclusion media will be described separately in the corresponding sections. Both the FEM and UDEC analyses assume that the calculation domain 200.0 cm × 100.0 cm (see Fig. 4) is restrained perpendicular to the plane of analysis (i.e., plane-strain case).

4.1. Effect of cavity on wave attenuation

To quantify the attenuation of blast wave due to a cavity in a rock shelter layer, a dimensionless variable, decay factor (DF), is defined as follows:

$$\text{DF} = \frac{\sigma_{x0} - \sigma_x}{\sigma_{x0}} \tag{16}$$

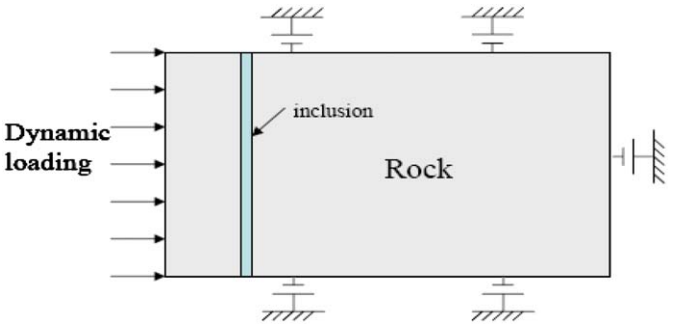

Fig. 4. Numerical model of P-wave propagating in rock shelter.

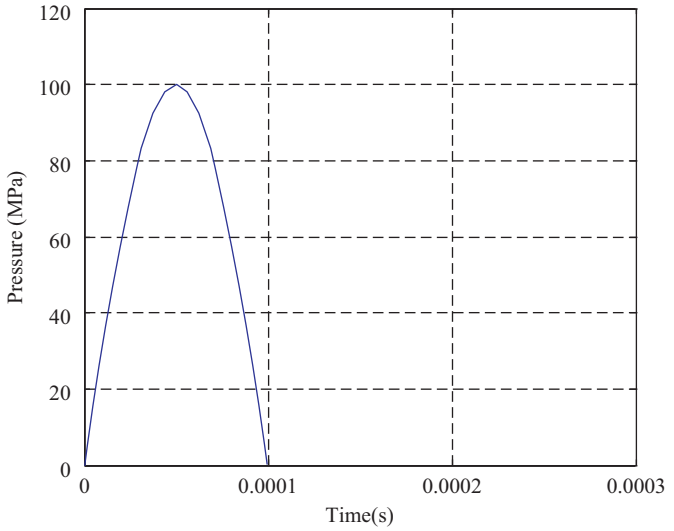

Fig. 5. Pressure–time curve for applied blast loading.

where σ_x represents the peak value of axial stress at a specified position (on the symmetric line and immediate after cavity) with a cavity in the rock, and σ_{x0} is the peak value of the same component at the same position without a cavity in the rock shelter layer. Eq. (16) indicates that a larger DF implies a superior attenuation effect.

It is assumed that the filled layer is free air corresponding to the foregoing case (i), namely $\rho_2 C_2 = 0$. Four widths (vertical dimension in the cross section, see Fig. 4) of rectangular cavity are chosen in the calculations: 0.2, 0.4, 0.8 and 1.0 m, respectively. The thickness (horizontal dimension) of the cavity is fixed at 0.2 m. The variations of decay factor with cavity width are shown in Fig. 6a. It can be seen that the DF rapidly increases with cavity width. For example, for a cavity width of 0.2 and 1.0 m, the corresponding decay factors for peak σ_x are 0.68 and 1.0, respectively. It is noticed that, when the rectangular cavity has the same width as the rock shelter, the attenuation effect is the best (DF = 1.0) because there is neither transmission nor diffraction of waves. However, such scenario is against the stability of whole defense structure. In practice, the width of cavity is usually shorter than that of rock shelter layer, and multiple continuous cavity inclusions are usually adopted, as illustrated in Fig. 1.

In another series of analyses, four values of thicknesses h are taken in the calculation: 0.02, 0.04, 0.06 and 0.08 m, respectively. The width of cavity is fixed at 0.4 m. Fig. 6b shows that the cavity thickness has little influence on the decay factor for the peak σ_x. As the cavity thickness increases, DF remains essentially the same.

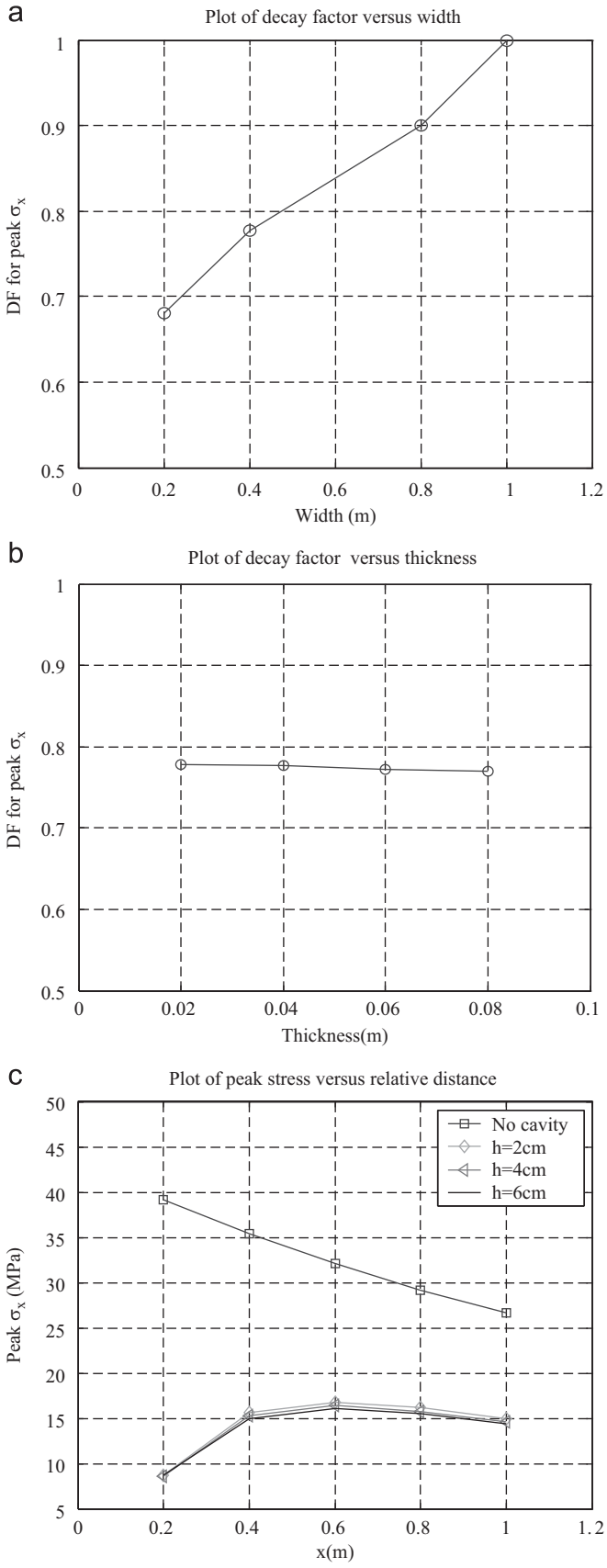

Fig. 6. Effect of cavity inclusion on wave attenuation, (a) plot of decay factor versus width, (b) plot of decay factor versus thickness and (c) plot of peak stress versus relative distance.

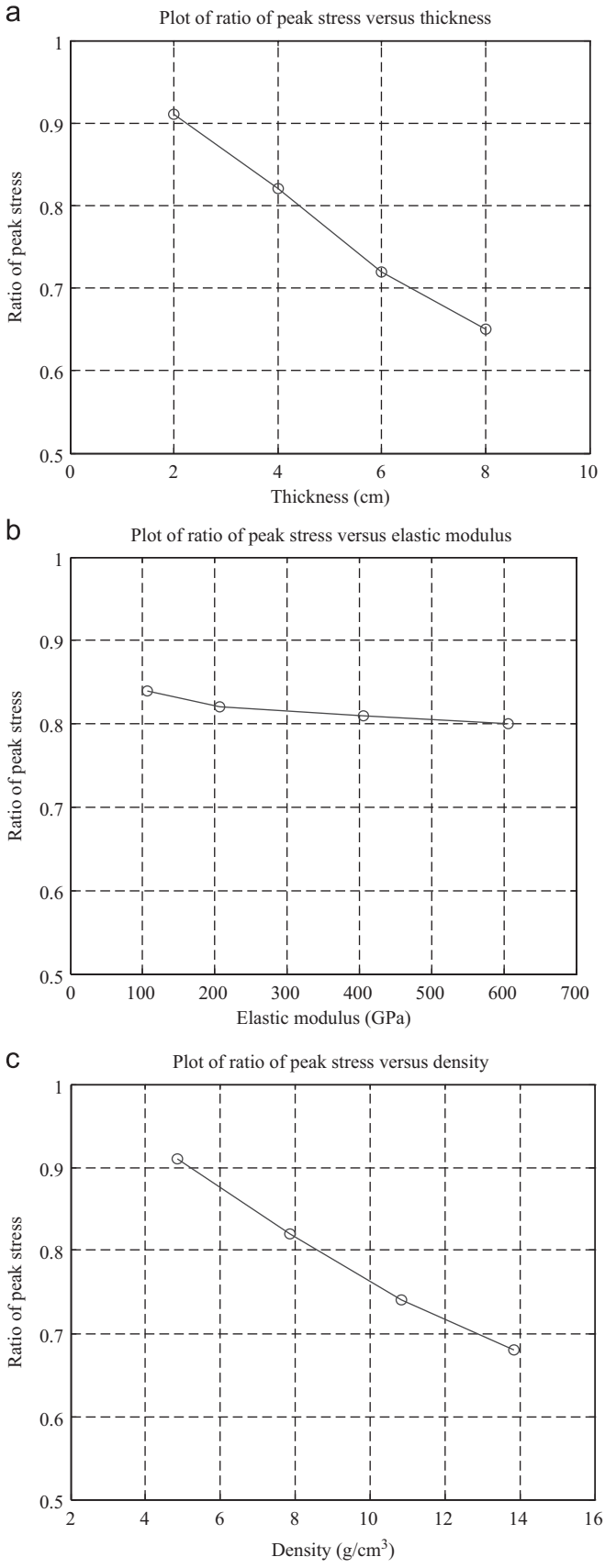

Fig. 7. Effect of steel-plate inclusion on wave attenuation, (a) plot of ratio of peak stress versus thickness, (b) plot of ratio of peak stress versus elastic modulus and (c) plot of ratio of peak stress versus density.

This phenomenon can be further corroborated in Fig. 6c, from which it can be found that the curves of peak axial stress are basically the same for all nonzero h values.

4.2. Effect of rigid body on wave attenuation

To facilitate the quantification of the analysis, the "rigid body" inclusion is approximated by a high strength steel plate in the present numerical simulation with the following typical properties: density $\rho = 7850.0\,\mathrm{kg/m^3}$, elastic modulus $E = 206.0\,\mathrm{GPa}$ and Poisson's ratio $\mu = 0.30$. All the numerical analysis results are plotted in Fig. 7. It is noted that, unlike the case of cavity inclusion, the thickness of steel-plate inclusion exerts substantial influence on wave transmission. When the thickness h increases from 0.02 to 0.08 m, the ratio of peak stress (immediate after to immediate before the inclusion) drops from 0.91 to 0.65. Clearly, the attenuation of wave increases with increasing the steel plate thickness. This may be attributable to the fact that, as the thickness of steel plate increases, the wave travels through a longer distance, resulting in more energy dissipation of waves.

It can be seen from Fig. 7b that the influence of elastic modulus on wave attenuation is smaller. For the present case, when the elastic modulus is increased by 6.0 times, the ratio of peak stress only decreases from 0.84 to 0.80. However, the density has great influence on the wave attenuation (see Fig. 7c). For instance, the ratio of peak stress is 0.91 when $\rho = 4.85\,\mathrm{g/cm^3}$, while it declines to 0.68 for $\rho = 13.85\,\mathrm{g/cm^3}$. This is because a higher density inevitably results in a higher wave impedance.

4.3. Effect of joint on wave attenuation

Joint is a common discontinuity in rock mass, and its presence plays an important part in the responses to either static or dynamic loading [22]. The effect of natural dry joint on wave propagation and attenuation in rock shelter layer is examined herein. The UDEC modelling is specially adopted, which has been recognized to be a better alternative for discontinuous problems [16].

Mohr–Coulomb slip joint model is assumed for the joint in calculations. This law works in a similar fashion both for contacts between rigid blocks and contacts between deformable blocks. Both shear and tensile failure are considered, and joint dilation is

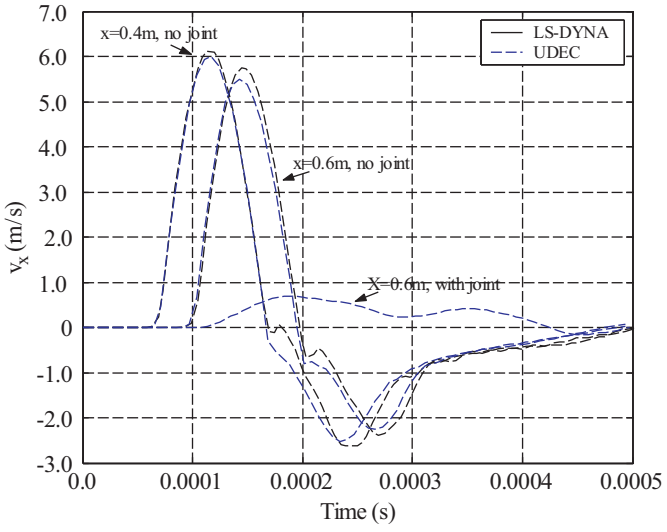

Fig. 8. Comparison of velocity histories in calculation domain.

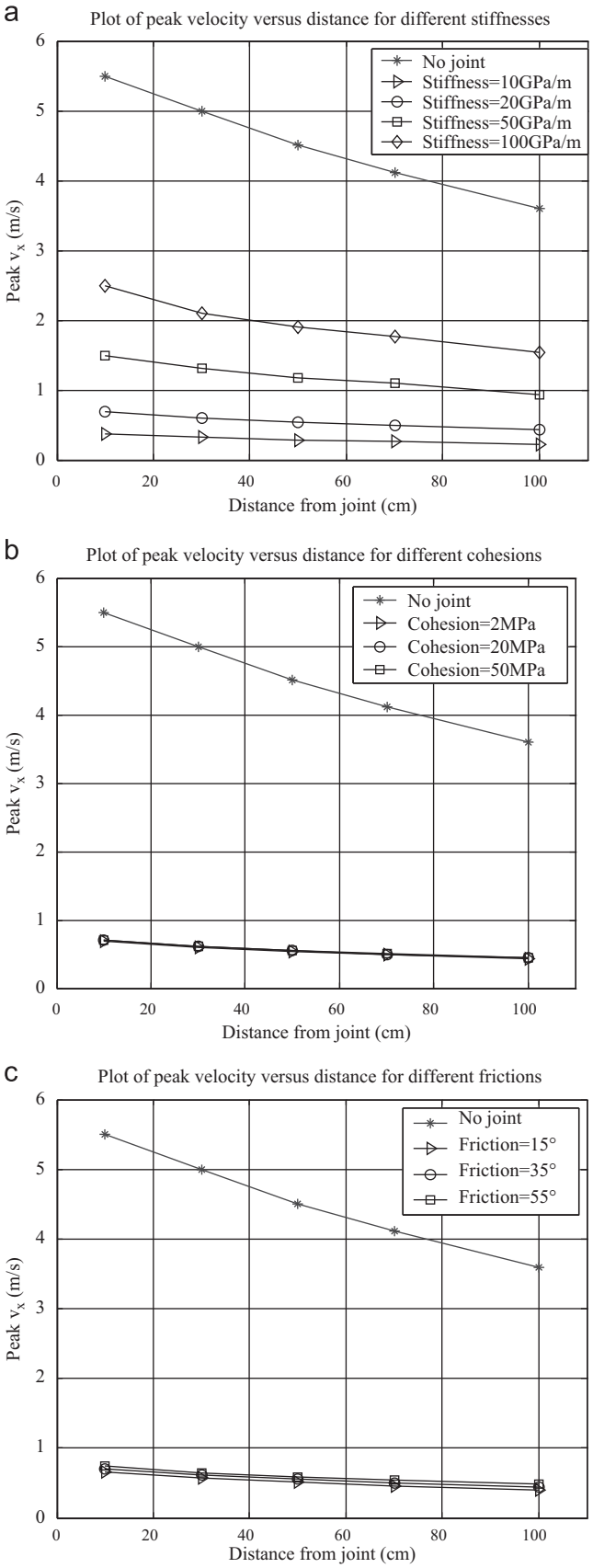

Fig. 9. Effect of joint inclusion on wave attenuation, (a) plot of peak velocity versus distance for different stiffnesses, (b) plot of peak velocity versus distance for different cohesions and (c) plot of peak velocity versus distance for different frictions.

also included [16]. Typical values are assumed for joint properties in the present analysis: normal stiffness $k_n = 20.0$ GPa, shear stiffness $k_s = 20.0$ GPa, cohesion $C = 2.0$ MPa, friction angle $\phi = 25.0^\circ$ and no tensile strength is considered.

The following equation can be used to estimate the applied velocity on the left non-reflecting boundary:

$$v_n = \frac{\sigma_n}{\rho C_p} \tag{17}$$

where $C_p = \sqrt{(K + 4G/3)/\rho}$ is the velocity of longitudinal wave with K and G being bulk and shear modulus.

Using Eq. (17), the applied maximum velocity is found to be 6.27 m/s, corresponding to a peak stress of 100.0 MPa.

Fig. 8 compares the numerical results of two different methods for the same problem without joints. It can be seen that the UDEC curves match the FEM ones very well, which also testifies that the handling of boundary conditions and the selection of element size in two numerical methods are accurate and consistent. As for the case with a joint inclusion, UDEC has to be resorted to and it can be noted in Fig. 8 that the wave across joint is greatly attenuated with the amplitude abruptly dipping from 5.5 to 0.69 m/s. Furthermore, great changes have come over the waveform, which is due to the back and forth reflection and interference of waves between the joint surface and the left boundary.

Fig. 9a shows the results obtained from different joint stiffness values. It is easy to see that joint stiffness has significant influence on wave attenuation. A joint of lower stiffness reflects more blast waves and causes greater wave attenuation due to its larger energy absorption capability. However, the cohesion and friction of joint are insensitive to wave attenuation. As shown in Fig. 9b and c, all the curves corresponding to various nonzero cohesions and frictions are practically identical.

5. Conclusions

The performance of an underground protective structure is a key issue in the design of civil defense engineering. This paper focuses on the propagation and attenuation of one-dimensional P-wave in rock shelter layer. The effect of single inclusion in rock shelter on wave attenuation is explored analytically. Then, the effects of three kinds of inclusions (cavity, rigid body and joint) on wave transmission and attenuation are numerically investigated and discussed via the finite element and distinct element modelling. Based on the present work, the following general conclusions may be drawn:

(1) With the assumption that an artificial inclusion is completely consolidated with the surrounding rock, the derived analytical formulae suggest a strong transmission of waves when the impedances are matching ($k = 1$), whereas the cavity ($k = 0$) and rigid body ($k \to \infty$) inclusions can greatly attenuate waves and may produce zero transmission.

(2) Cavity width exerts significant influence on wave attenuation in the area behind the inclusion, while the thickness has little impact. A larger width can preferably attenuate and even obstruct the diffraction of waves. Nevertheless, the selection of cavity width should take account of structural stability.

(3) Rigid body inclusion like steel plate can fairly well dissipate wave energy due to its higher wave impedance compared to adjoining rock. Increasing density or thickness in the appropriate range is superior to the increment of elastic modulus for the attenuation of blast waves.

(4) For a joint inclusion of lower stiffness, larger deformation and energy absorption arise. The strong influence of joint stiffness on wave propagation is inspected via UDEC modelling. On the

other hand, the effects of joint cohesion and friction are found to exert little effects on the wave attenuation.

Acknowledgements

This study was supported by the Specialized Research Fund for the Doctoral Program of Higher Education (No. 20070358073), the Program for New Century Excellent Talents in University (No. NCET-08-0525), the Alexander von Humboldt Foundation and the Civil Aeronautics Joint Research Foundation (No. 60776821).

References

[1] Rohani B. Shielding methodology for conventional kinetic energy weapons. Technical report SL-8f-8. US army engineers corps, waterways experimental station, Vicksburg. M.S; 1987.
[2] Wang ZL, Li YC, Wang JG, Shen RF. A study of tensile damage and attenuation effect of perforated concrete defense layer on stress waves. Engineering Structures 2007;29(6):1025–33.
[3] Yang Z. Finite element simulation of response of buried shelters to blast loadings. Finite Elements in Analysis and Design 1997;24(3):113–32.
[4] Wang ZL, Wang JG, Li YC, Leung CF. Attenuation effect of artificial cavity on air-blast waves in an intelligent defense layer. Computers and Geotechnics 2006;33(2):132–41.
[5] Wang LL, Zhu ZX. Foundation of stress wave. Beijing: National Defense Industry Press; 1985 [in Chinese].
[6] Wang ZL, Li YC, Shen RF. Numerical simulation of tensile damage and blast crater in brittle rock due to underground explosion. International Journal of Rock Mechanics and Mining Science 2007;44(5):730–8.
[7] Gautam CK. Analytical and experimental evaluation of a buried shelter. Defense Science Journal 2007;57(2):299–307.
[8] Kenedey RP. A review of procedure for the analysis and design of concrete structure to resisting missile impact effects. Nuclear Engineering 1976;37(2):183–203.
[9] Hinman E. Shock response of underground structures to explosion, In: Eighth International Conference on Vibration and Shock, Lyons, France; 1988.
[10] Weidlinger P, Hinman E. Analysis of underground protective structure. Journal of Structural Engineering 1988;114(7):1658–73.
[11] Wang ZL, Li YC, Wang JG. Study of stress waves in geomedia and effect of a soil cover layer on wave attenuation using a 1-D finite difference method. Computer & Geosciences 2006;32(10):1535–43.
[12] Balandin DY, Bolotnik NN, Pilkey WD. Optimal protection from impact, shock, and vibration. Gordon and Breach Science Publishers; 2001.
[13] Kattis SE, Polyzos D, Beskos DE. Modelling of pile wave barriers by effective trenches and their screening effectiveness. Soil Dynamics and Earthquake Engineering 1999;18(1):1–10.
[14] Yao L. Evolution mechanism of stress waves and its application in defense engineering. Dissertation for Ph.D. University of Science and Technology of China; 2005.
[15] Li YC, Wang XJ, Hu XZ. Study on layered design and its defending function. Technical report of national defense engineering, USTC, China; 2004.
[16] Wang ZL, Li YC, Wang JG. Numerical analysis of attenuation effect of EPS geofoam on stress-waves in civil defense engineering. Geotextiles and Geomembranes 2006;24(5):265–73.
[17] Livermore Software Technology Corporation (LSTC). LS-DYNA keyword user's manual (CA, USA); 2003.
[18] Itasca Consulting Group, Inc. UDEC-Universal Distinct Element Code. Version 4.0, User Manual, Minnesota, USA; 2004.
[19] Hallquist JO. LS-DYNA theoretical manual. Livermore, CA: Livermore Software Technology Corporation; 2003.
[20] Li YC, Yao L, Hu XZ, Cao JD, Deng J. Some problems on jump conditions of shock waves in 3-dimensional solids. Applied mathematics and mechanics (English edition) 2006;27(2):187–94.
[21] Hu XW, Zhu RG, Cheng K. Study on the interaction between P-wave and groove filled medium. Blasting 2002;19(3):4–7 [in Chinese].
[22] Hudson JA, Harrison JP. Engineering rock mechanics. Amsterdam: Pergamon; 1997.